AGU PUBLICATIONS

JGR

Journal of Geophysical Research: Earth Surface

RESEARCH ARTICLE

10.1002/2016JF003864

Key Points:
- Soil chemistry and weathering vary nonlinearly across a large rainfall gradient (400–4700 mm/yr) in NZ
- Climate control evidenced in detailed soil chemistry, Fe and Al mobilities, and cation leaching
- Moisture availability can act as a "switch" to enable rapid chemical weathering in young soils

Supporting Information:
- Supporting Information S1
- Data Set S1

Correspondence to:
J. L. Dixon,
jean.dixon@montana.edu

Citation:
Dixon, J. L., O. A. Chadwick, and P. M. Vitousek (2016), Climate-driven thresholds for chemical weathering in postglacial soils of New Zealand, *J. Geophys. Res. Earth Surf.*, *121*, 1619–1634, doi:10.1002/2016JF003864.

Received 18 FEB 2016
Accepted 12 AUG 2016
Accepted article online 17 AUG 2016
Published online 16 SEP 2016

©2016. The Authors.
This is an open access article under the terms of the Creative Commons Attribution-NonCommercial-NoDerivs License, which permits use and distribution in any medium, provided the original work is properly cited, the use is non-commercial and no modifications or adaptations are made.

Climate-driven thresholds for chemical weathering in postglacial soils of New Zealand

Jean L. Dixon[1,2], Oliver A. Chadwick[2], and Peter M. Vitousek[3]

[1]Department of Earth Sciences and the Institute on Ecosystems, Montana State University, Bozeman, Montana, USA, [2]Department of Geography, University of California, Santa Barbara, California, USA, [3]Department of Biology, Stanford University, Stanford, California, USA

Abstract Chemical weathering in soils dissolves and alters minerals, mobilizes metals, liberates nutrients to terrestrial and aquatic ecosystems, and may modulate Earth's climate over geologic time scales. Climate-weathering relationships are often considered fundamental controls on the evolution of Earth's surface and biogeochemical cycles. However, surprisingly little consensus has emerged on if and how climate controls chemical weathering, and models and data from published literature often give contrasting correlations and predictions for how weathering rates and climate variables such as temperature or moisture are related. Here we combine insights gained from the different approaches, methods, and theory of the soil science, biogeochemistry, and geomorphology communities to tackle the fundamental question of how rainfall influences soil chemical properties. We explore climate-driven variations in weathering and soil development in young, postglacial soils of New Zealand, measuring soil elemental geochemistry along a large precipitation gradient (400–4700 mm/yr) across the Waitaki basin on Te Waipounamu, the South Island. Our data show a strong climate imprint on chemical weathering in these young soils. This climate control is evidenced by rapid nonlinear changes along the gradient in total and exchangeable cations in soils and in the increased movement and redistribution of metals with rainfall. The nonlinear behavior provides insight into why climate-weathering relationships may be elusive in some landscapes. These weathering thresholds also have significant implications for how climate may influence landscape evolution and the release of rock-derived nutrients to ecosystems, as landscapes that transition to wetter climates across this threshold may weather and deplete rapidly.

1. Introduction

1.1. Climate's Elusive Control on Chemical Weathering

Soils lie at the interface of air, water, life, and rock, and the weathering dynamics that transform minerals and water in soils are shaped by diverse processes. Climate has long been recognized to be one of the major drivers of these weathering processes [*Jenny*, 1941]. Temperature controls the kinetics of chemical reactions, and water has a role in nearly every chemical weathering reaction that directly results in mass loss from a rock or mineral. Therefore, warmer and wetter conditions should lead to higher weathering rate and intensity in soils. However, a coherent understanding of how climate controls soil chemical weathering remains elusive. Several reasons emerge for the lack of consensus across studies.

1.2. Competing Variables

First, while the conceptual framework for climate control on weathering rates is validated by laboratory experiments quantifying dissolution rates under different temperature or water-flow conditions [*White et al.*, 1999; *White and Brantley*, 2003], field-based studies reveal significant complexity among climate-weathering linkages [*Brantley*, 2003; *Drever et al.*, 1994; *White and Brantley*, 2003], which may be explained by time-dependent factors such as changing mineral surface area, pore water concentrations, and secondary precipitates. Similarly, climate's control on soil weathering can be modified by the complex influence of other competing variables such as lithology, erosion rates, and/or dust deposition [e.g., *Ferrier et al.*, 2012; *Riebe et al.*, 2004]. Furthermore, field-based weathering rates are often measured in locations where multiple variables (including climate variables such as temperature and water availability) exert competing controls on mineral weathering and the fate of released ions [*Chadwick and Chorover*, 2001]. These competing climatic controls may be deconvolved using careful sampling designs and accounting for multiple variables [e.g., *Dixon et al.*, 2009a; *Rasmussen et al.*, 2011; *White and Blum*, 1995]; however, derived relationships and models may be site specific or have limited applicability.

1.3. Different Perspectives, Different Metrics, and Different Systems

Second, disparate communities within the Earth sciences probe the question of climate control on weathering from different perspectives and using different metrics. A number of geomorphologists and geochemists have sought insight by exploring the role of climate in actively eroding landscapes. Partially motivated by the recognition that silicate weathering in mountain belts may modulate global climate [e.g., *Walker et al*., 1981], past research has looked for a climate control on net chemical weathering rates [e.g., *Dixon et al*., 2009b; *Ferrier et al*., 2012; *Larsen et al*., 2014; *Riebe et al*., 2004]. Contrary to original expectations, this research finds that globally, net weathering rates correlate more strongly with erosion rates than climate variables such as mean annual precipitation or temperature [e.g., *Dixon and von Blanckenburg*, 2012; *West et al*., 2005]. Indeed, physical erosion is particularly important in controlling weathering rates via its control on mineral residence times within the surface weathering environment [*Riebe et al*., 2004], and these links have been confirmed in detail in soils [e.g., *Dixon et al*., 2009a; *Ferrier et al*., 2012; *Riebe et al*., 2004] and stream sediments and solutes [e.g., *Stallard and Edmond*, 1983; *West et al*., 2005].

Emerging in response to these field-based studies, numerical models based on chemical reaction kinetics and mineral residence times [*Ferrier and Kirchner*, 2008; *Gabet and Mudd*, 2009; *Hilley et al*., 2010; *Waldbauer and Chamberlain*, 2005] provide key insights into the conditions where climate might control weathering rates. These models predict that erosion may either enhance or diminish weathering reactions by exposing new minerals for weathering (supply-limitation weathering) or by reducing mineral residence times within the surface weathering reactor (kinetic-limitation weathering). These models predict that climate (via moisture and temperature) should directly influence weathering rates only if those rates are kinetically limited. To conceptualize this relationship, imagine a slowly eroding landscape mantled by thick soils. As a fragment of rock is exhumed from depth via surface erosion, weatherable minerals are lost from that rock and more inert minerals remain in the weathered soil residuum. In a supply-limited weathering system, the mineral residence time is sufficiently long that the rate of weathering is set solely by the supply rate of new weatherable minerals. Therefore, in these systems weathering should be insensitive to increases in moisture availability or temperature. For example, weathering in tropical Sri Lanka is remarkably slow for its warm and wet climate, largely due to slow mineral supply rates [*Hewawasam et al*., 2013]. Conversely, climate should exert considerable direct control on weathering rates in systems with relatively short residence times, where abundant weatherable minerals are available to react with passing pore waters. Most studies that have explored climate-weathering relationships in soils have shown evidence of supply-limited weathering [*Dixon and von Blanckenburg*, 2012; *Riebe et al*., 2004; *Riebe et al*., 2001], although there is some indication that both erosion and moisture availability may regulate weathering fluxes in kinetically limited systems where mineral residence times are relatively short [e.g., *Rasmussen et al*., 2011; *West et al*., 2005].

In contrast to those studies that focus primarily on net weathering rates, which generally seem insensitive to climate across widely diverse landscapes, a number of other soil and biogeochemical studies have found that weathering indices can change dramatically with climate variables—specifically with changes in moisture availability. For example, *Ewing et al*. [2006] found that soils in the Atacama desert of Chile experienced large chemical and physical changes at the hyperarid-arid climate transition. Strong gradients in the contribution of atmospheric salts were seen across this threshold, which also drove changes in weathering and soil production rates. Along climate gradients in the Sierra Nevada of California, iron mobility and clay chemistry and abundance varied with rainfall [*Dahlgren et al*., 1997], as did other indices of chemical weathering [*Rasmussen and Tabor*, 2007]. Abundant work in Hawaii found systematic variability in the geochemistry of very slowly eroding soils across gradients in rainfall [*Chadwick et al*., 2003; *Vitousek and Chadwick*, 2013]. These authors observed dramatic changes within Hawaiian soils with respect to bulk elemental chemistry and the mobility, redistribution and loss of metals, and labile cations. Furthermore, these chemical changes occurred rapidly across a narrow portion of the rainfall gradient, indicating that water availability causes thresholds for soil weathering (see discussion by *Chadwick and Chorover* [2001]).

Many of these strong changes in soil weathering mentioned above are observed in soil systems with long residence times (150 ka–4 Ma in the case of Hawaii) and emerge only by detailed analysis of soil chemistry and elemental mobility. Therefore, it is difficult to resolve these studies with those from the geomorphic community that generally suggest that climate control on net weathering should be most evident in young mountainous systems. How do we reconcile these disparate observations about the role of climate in

controlling weathering status and element fluxes across Earth's surface? More work is needed that considers climate controls on weathering and soil development from both geomorphic and soil science perspectives. Unfortunately, there are too few data-rich studies that provide both geomorphic context and detailed soil geochemistry. Two critical research questions emerge from this synthesis of previous studies across different fields:

1. Can we observe moisture control on chemical weathering in young soils where other controlling factors are constrained?
2. What is the nature of this control, and do these systems display pedogenic thresholds similar to those observed in older soils?

In this study, we combine insights and approaches from across the soil-science, biogeochemistry, and geomorphology communities to tackle the fundamental question of how moisture availability influences soil chemistry and formation. To address these questions, we quantify pedogenic changes in young, noneroding, postglacial soils of New Zealand, exploring soil elemental geochemistry along a large precipitation gradient. Our exploration of climate control on chemical weathering and soil development focuses on young soils for two reasons: (1) according to previous numerical modeling and data [e.g., *Dixon et al*., 2012] young soils may be the most geomorphically relevant for understanding climate controls on soil formation and (2) these soils should provide insight into the persistence and occurrence of geochemical thresholds observed in older, more stable landscapes such as Hawaii [*Vitousek and Chadwick*, 2013].

2. Approach

2.1. Study Area

Our field area is situated along a 60 km stretch of the N-S trending Waitaki Valley on Te Waipounamu, the South Island of New Zealand (Figure 1). A strong rainfall gradient is established by orographic effects along the Southern Alps Range, which marks the NW boundary of our study area. Complex collision between the Indo-Australian Plate and the Pacific Plate is expressed along the Alpine Fault, which traces the western edge of the Southern Alps. Dominant westerly winds bring moist air to the west coast of New Zealand, and a strong rainfall gradient develops leeward and southward of the Southern Alps. Modern precipitation rates decrease from approximately 14,000 mm/yr near the crest of the Alps (north of the study area) to as low as 200 mm/yr in the center of the island. We present two sources of precipitation data (Table 2). The National Institute of Water and Atmospheric Research (Taihoro Nukuwange) provides detailed raw and statistical climate data across New Zealand (*NIWA CliFlo*) and maintains a geographic information system-based database of 30 year precipitation averages (1970–2000) that spans the entire study area (Figure 1). In addition, work by *Kerr* [2009] refined these averages across a portion of the study area, using improved statistical and time series analysis of an expanded set of precipitation gauges. From these data, we observe large changes in precipitation from NW to SE across the study area, which are accompanied by much lesser changes in elevation (~370–1200 m). The maximum/minimum annual temperatures across the region vary from only 3.9/9.4°C in the southern region near Lake Benmore to 3.7/13.8°C in the northern region near Mt. Cook (*NIWA CliFlo*). Gradients in precipitation are complemented by changes in water deficit and water balance, as reported by the Ministry of the Environment for New Zealand [*Leathwick et al*., 2002]. Annual water deficit represents the degree to which potential evapotranspiration exceeds water availability. Water deficit values across the study area range from 0 mm/yr (reflecting sites with a positive water balance) to ~280 mm/yr (reflecting a low annual precipitation and negative water balance; Table 2).

To isolate the role of climate, we selected grassland sites that minimize variation in soil age, erosion rates, and lithology. Vegetation across all sample sites is dominated by tussock grasses (*Festuca novae-zelandiae* and *Agrostis capillaris*) and small herbaceous plants [*Webb et al*., 1986]. In addition, we recognize that the present grassland vegetation represents a response to human modification of prehuman forest ecosystems. Vegetation type and productivity covary with climate and are treated here as part of the overall climate control on soil processes. Soils are developed in wind-derived loess, which is deposited on glacial deposits of known age [*Amos et al*., 2007; *Barrell et al*., 2011; *Putnam et al*., 2010; *Schaefer et al*., 2006]. Moraine ages, dated using in situ cosmogenic ^{10}Be [*Schaefer et al*., 2006], range from 12.6 to 19.7 kyr. Four sets of moraines flank the Lake Pukaki region of the Waitaki Valley, just south of Mt. Cook/Aoraki. We restrict our sample sites to loess deposited on pre-Holocene Last Glacial Maximum (LGM; Tekapo Formation) and post-LGM

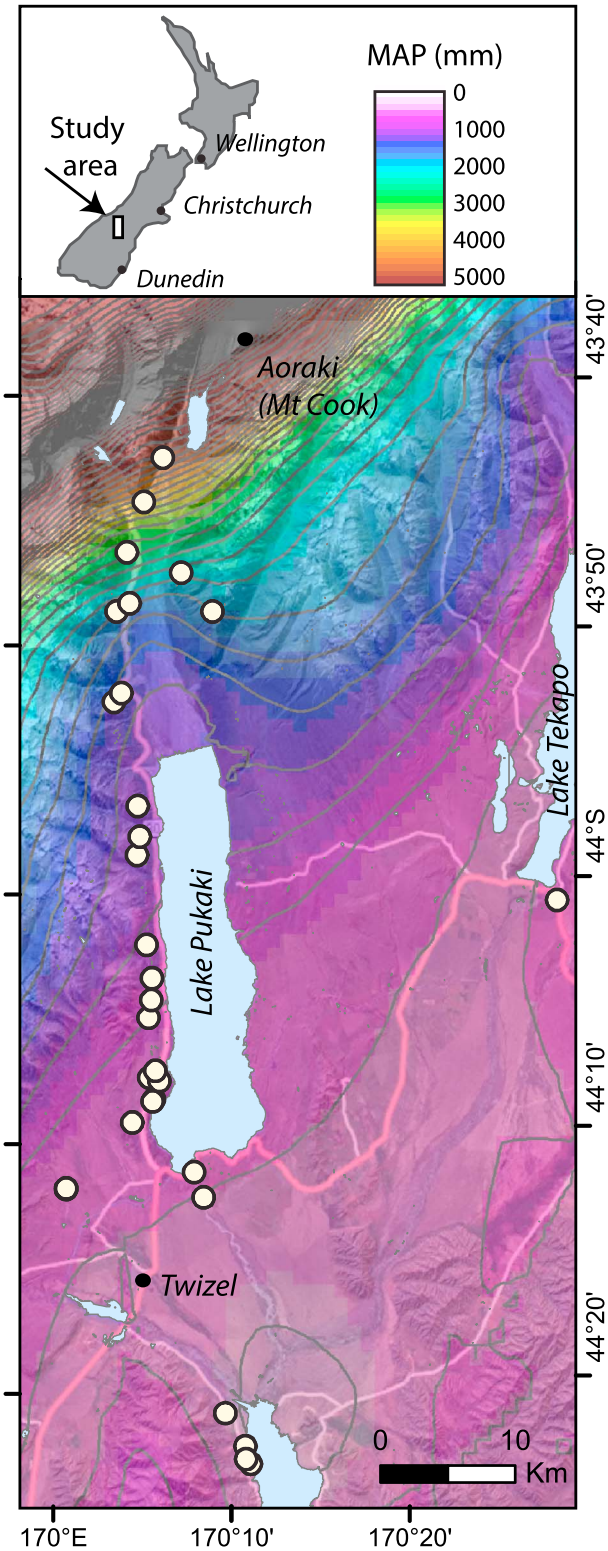

Figure 1. Loess-derived soils were sampled atop LGM and post-LGM moraines and outwash terraces along the Waitaki drainage in the South Island of New Zealand. The sites span a large precipitation gradient, from ~400 mm/yr in the south to upward of 4700 mm/yr in the northern sites located near Mt. Aoraki. The map shows the mean annual precipitation (from *NIWA CliFlo*), contoured at 200 mm/yr increments.

(Birch Hill Formation) moraines and outwash. The loess and its underlying till are carbonate poor and derived from greywacke and argillite bedrock of the Torlesse Supergroup, which is a component of uplifted Mesozoic turbidite sequences [*Eden and Hammond*, 2003; *Raeside*, 1964]. These parent rocks yield a loess mineral assemblage including quartz, K-feldspar, muscovite, plagioclase, and minor chlorite [*Spörli and Lillie*, 1974; *Webb et al.*, 1986].

Glacial deposit ages of ~12.6 ka provide an upper constraint on soil age and the timing of loess deposition and stabilization. Rapid loess deposition likely followed deglaciation, and the post-LGM period is broadly associated with landscape stability and vegetation establishment. However, temporal variation during the Holocene in the strength of the westerlies and seasonal rainfall resulted in large changes in paleoenvironmental conditions [*McGlone*, 1995; *McGlone et al.*, 1995], which are likely linked to multiple periods of soil stability and instability across the region. Although dust accumulation rates have not been calculated along our specific gradient, previous estimates from elsewhere in the South Island have placed loess accumulation at approximately 0.22 mm/yr for the period between 11.7 and 5.5 ka [*Berger et al.*, 1996]. Based on paleoecology and inferred dust accumulation rates, weathering of loess-derived soils in our study region initiated with surface stabilization, establishment of vegetation, and the change to wetter conditions during the early to middle Holocene. Therefore, although loess deposition may have been pulsed at the end of the LGM, we predict soil residence times of ~8–6 ka, reflecting the period of declining loess deposition, increased moisture, and soil stability.

2.2. Field Sampling

Previous work in this region measured pedogenic variation across four soil profiles, widely spaced along the Waitaki climate gradient [*Webb et al.*, 1986].

Table 1. Parent Material Chemistry

Sample No.	Si (%)	Al (%)	Fe (%)	Ca (%)	Mg (%)	Na (%)	K (%)	Ti (%)	Zr (ppm)
Buried loess a	30.39	7.04	3.26	1.97	0.84	1.65	1.56	0.41	236.07
Buried loess b	27.97	7.93	3.56	1.62	0.99	1.82	1.75	0.42	237.07
Buried Loess c	29.21	7.49	3.32	1.68	0.88	1.80	1.69	0.39	238.07
Fine glacial outwash	30.29	7.63	3.09	1.43	0.96	2.18	2.30	0.36	230.07
Mean ± standard error	29.47 ± 0.57	7.52 ± 0.19	3.31 ± 0.10	1.67 ± 0.11	0.92 ± 0.04	1.86 ± 0.11	1.82 ± 0.16	0.39 ± 0.01	235.3 ± 1.8

Characterization of these four profiles provided key insight into the range of chemical variability and allowed us to target detailed sampling to determine the nature of the chemical transitions among the existing profiles. We sampled 28 soil profiles in thin (~1 m) loess deposits that mantle moraines and outwash in the Waitaki catchment, extending from Lake Benmore in the south to just below the Tasman glacier in the north (Figure 1). Sites span ~64 km across a large S-N gradient in mean annual precipitation, from ~400 to 4700 mm/yr [*Kerr*, 2009]. Each site is situated on the flat upper surfaces of moraines (and abandoned outwash fans in the southern portion of the study area), with local slope gradient less than 3° and located away from high-gradient moraine side slopes. Overall, these sample sites represent subtle (nearly imperceptible) concavities within convexities in the landscape. In this way we minimized the amount of soil surface loss by runoff and the amount of surface gain by run-on. In order to avoid postdepositional reworking of loess that would produce local variations in soil depth, each site was investigated using multiple auger holes to determine average depths and identify a representative sample profile.

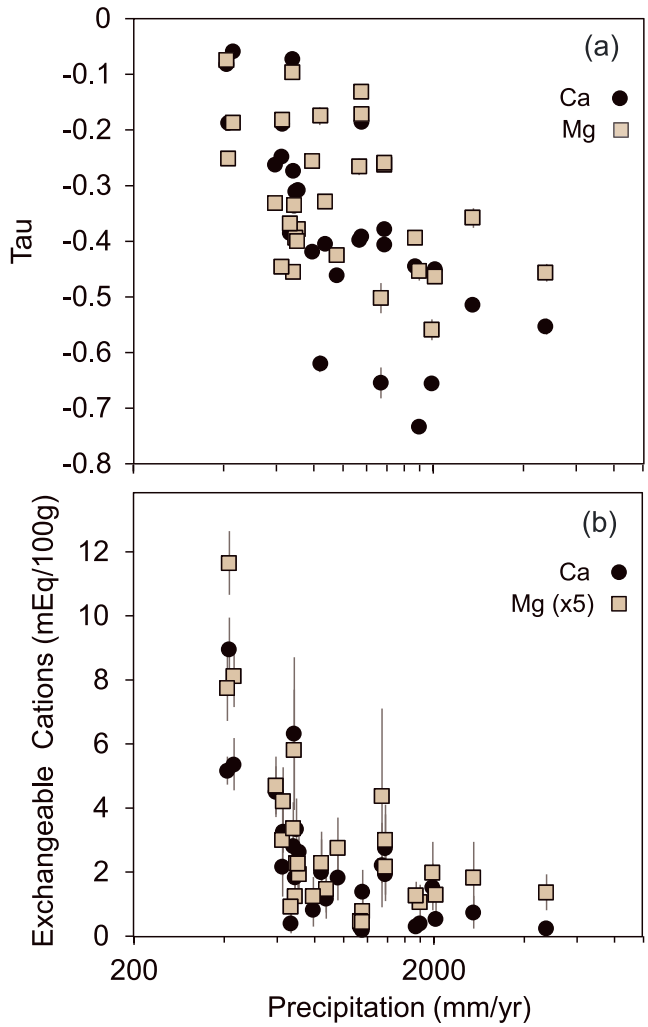

Figure 2. (a) Depth-averaged Ca and Mg Tau values from 28 soil profiles show increasing losses of cations with increasing mean annual precipitation, with significant scatter (TauCa $r^2 = 0.21$; TauMg $r^2 = 0.51$). (b) Exchangeable, plant-available forms are rapidly and nonlinearly depleted with increasing precipitation. The error bars on depth-weighted averages represent the standard error throughout each profile. Values for exchangeable Mg are multiplied by a factor of 5 to plot with Ca values. Logarithmic *x* axes highlight how chemical changes occur across a narrow range in precipitation. The nonlinearity of this decrease even when presented on a logarithmic axis also highlights the threshold behavior of this decrease.

Soil was collected from each of the 28 profiles by integrated sampling every 10 cm from the soil surface to the base contact with coarse glacial till. We collected and preserved soil "clods" for bulk density analysis. Soil descriptions, including texture and color, were recorded in the field for each soil horizon within a profile. The sampled soils range from about 40 to 150 cm in depth to the clear contact with glacial till, with most being 60 to 70 cm.

To provide some constraints on the soil parent material, we collected three samples of loess material from ~4 m depth in an anomalously thick deposit along Lake Benmore in the southern region of the study area. This deep loess

Table 2. Soil Profile Elemental Depletions

Profile No.	Depth (cm) [a]	Map 1 (mm) [b]	Map 2 (mm)[c]	Annual Water Deficit (mm)[d]	Depth-Weighted Average Tau Values[e]							
					τ_{Si}	τ_{Al}	τ_{Fe}	τ_{Ca}	τ_{Mg}	τ_{Na}	τ_{K}	τ_{P}
43	50	408	-	276	−0.01	0.02	−0.04	−0.08	−0.07	−0.08	−0.01	0.01
14	60	414	-	240	−0.04	−0.05	−0.20	−0.18	−0.25	−0.16	−0.19	0.25
15	30	429	-	278	0.00	−0.02	−0.10	−0.06	−0.18	−0.10	−0.04	0.16
41	45	593	-	151	0.20	−0.05	−0.19	−0.26	−0.33	0.16	0.00	0.49
16	65	623	-	133	0.28	−0.04	−0.28	−0.25	−0.44	0.20	−0.08	0.21
19	50	626	-	182	0.18	0.03	−0.10	−0.19	−0.18	0.13	−0.10	0.99
40	60	665	-	124	0.05	−0.07	−0.23	−0.38	−0.37	−0.04	−0.30	−0.10
17	60	677	-	141	0.17	0.11	−0.08	−0.07	−0.09	0.33	0.20	0.48
13	35	681	804	124	0.20	−0.06	−0.23	−0.27	−0.45	0.09	−0.11	0.51
12	40	686	-	123	0.11	−0.06	−0.19	−0.33	−0.33	0.01	−0.11	0.55
11	30	693	823	117	0.13	−0.05	−0.19	−0.31	−0.39	0.03	−0.13	0.31
25	40	702	-	102	0.07	−0.06	−0.16	−0.38	−0.40	−0.05	−0.15	0.51
10	30	707	842	106	0.10	−0.08	−0.20	−0.31	−0.38	0.00	−0.16	0.37
24	70	788	943	56	0.10	0.05	−0.06	−0.42	−0.25	−0.08	0.05	0.19
9	80	840	965	46	−0.13	0.10	−0.03	−0.62	−0.17	−0.35	0.16	0.26
23	50	871	1011	31	0.03	−0.06	−0.13	−0.40	−0.33	−0.07	−0.21	0.42
8	40	953	1059	9	−0.02	−0.11	−0.14	−0.46	−0.42	−0.18	−0.18	0.31
5	80	1132	1329	0	−0.01	−0.04	−0.09	−0.40	−0.26	−0.20	−0.08	−0.07
21	100	1149	1503	0	−0.07	0.00	−0.09	−0.39	−0.13	−0.17	0.04	−0.06
4	110	1152	1403	0	0.16	0.01	−0.07	−0.18	−0.17	0.03	0.14	0.21
6	50	1337	2036	0	−0.16	−0.12	−0.11	−0.65	−0.50	−0.37	−0.29	0.51
32	95	1373	2065	0	0.12	0.06	0.00	−0.38	−0.26	−0.08	0.06	−0.06
45	35	1737	1942	0	0.06	−0.06	−0.13	−0.44	−0.39	0.00	−0.22	0.13
22	70	1790	2551	0	−0.08	−0.08	−0.02	−0.73	−0.45	−0.33	−0.14	−0.11
7	55	1973	2420	0	−0.02	−0.11	−0.22	−0.65	−0.56	−0.20	−0.26	−0.11
44	73	2022	2444	0	0.04	−0.09	−0.20	−0.45	−0.46	0.01	−0.18	0.06
31	70	2702	3079	0	0.02	−0.03	−0.03	−0.51	−0.36	−0.09	−0.18	−0.07
30	70	4725	4387	0	0.07	−0.01	−0.08	−0.55	−0.45	−0.03	−0.14	−0.07

[a]Loess depth to top of glacial till.
[b]Mean annual precipitation as reported by (1) *NIWA CliFlo*: 30 year (1971–2000) climate averages. These data are shown in Figure 1.
[c]Mean annual precipitation as reported by (2) *Kerr* [2009].
[d]Annual water deficit reported from Land Environments of New Zealand classification (LENZ; data.mfe.govt.nz/layers/?q=LENZ) and the Ministry of the Environment for New Zealand [*Leathwick et al.*, 2002].
[e]Tau values calculated from ash-corrected molar concentrations using Ti as the immobile element. The negative values represent the elemental net loss.

material was preferable to samples collected at profile sites because unaltered loess parent material was not found in the thin soils across most of the study area. A fourth parent material sample was collected from fine sediment from the outwash plain of Tasman Glacier in the northernmost portion of the study area.

2.3. Soil Chemical and Physical Analyses

Samples were air dried and sieved to remove the >2 mm fraction. Because these soils are loess derived, this coarse fraction constitutes a trivial component (<0.1%) of all samples except those at the base of the soil profile and boundary with glacial till. Particle-size analysis, pH, and cation extractions were performed at University of California, Santa Barbara on subsamples of each of the 220 soil depth samples and four parent material samples. Particle-size analysis was performed using a CILAS 1190 laser particle-size analyzer, which measures the 0.04–2500 μm grain-size spectrum of unconsolidated soils and sediments in a liquid slurry. Concentrations of exchangeable Ca, Mg, Na, and K and the cation exchange capacity (CEC) were measured after sample extraction using NH_4OAC buffered at pH 7. Pedogenic iron and aluminum were measured using two sets of standard extraction techniques [e.g., *Burt*, 2004; *Miller et al.*, 2001]: an ammonium acid oxalate extraction to separate noncrystalline forms of Fe and Al and a dithionite-citrate-bicarbonate extraction to remove all pedogenic Fe and associated Al. Major element concentrations in the <2 mm size fraction were analyzed with X-ray fluorescence by ALS Chemex following lithium borate fusion, and Zr was measured by pressed pellet XRF. Loss on ignition (LOI) was determined following combustion of a 5 g aliquot at 1000°C for 1 h. Resin-extractable phosphorus (P) was measured at Stanford University using standard anion-exchange resin methods [*Vitousek et al.*, 2004] and analyzed on an Alpkem RFA/2 AutoAnalyzer. Total carbon

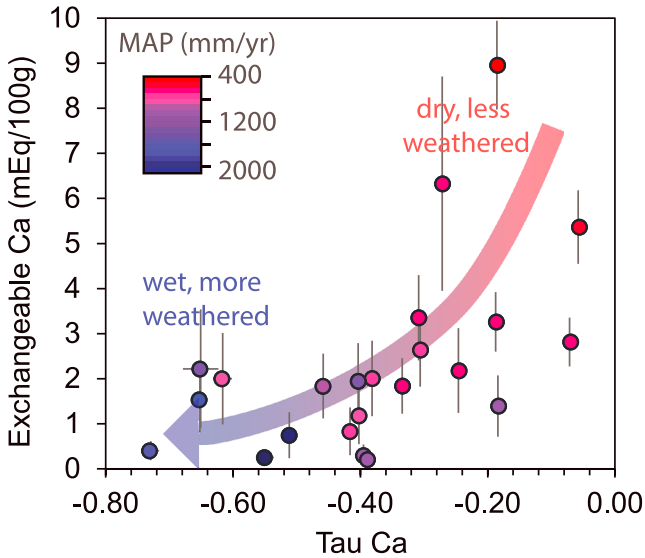

Figure 3. At intensely weathered wet sites, both net Ca and exchangeable, plant-available Ca become increasingly depleted (data same as shown in Figures 2a and 2b). Thus, cations are stripped from soil exchange sites at the same time primary minerals are weathering. These dual losses of Ca from total and exchangeable pools are complemented by increases in mean precipitation (shown by color gradient of symbols from red to purple).

and nitrogen were measured using a Carlo Erba NA 1500 elemental analyzer. Detailed methodology for P, N, C, and elemental extractions are described further in the electronic supplement to *Vitousek et al.* [2004].

Elemental concentrations in soils are indexed to loess parent material, and gains and losses of elements by weathering processes are represented as tau values (τ_i) or mass transfer coefficients [*Chadwick et al.*, 1990]. These values portray fractional mass gain ($\tau > 0$) or loss ($\tau < 0$) of mobile elements (i) in soil (subscript *w*) relative to parent material (subscript *p*) using an immobile, refractory element:

$$\tau_i = \left(\frac{i_w \times \mathrm{Ti}_p}{i_p \times \mathrm{Ti}_w} - 1\right).$$

Parent material elemental concentrations were derived from the average chemistry of four parent material samples (data presented in section 4.1). We chose to use Ti rather than Zr as the immobile element for tau calculations because Zr concentrations were highly variable with depth in our soil profiles, likely reflecting zircon variability during dust deposition, which could obscure any Zr enrichment or depletion due to weathering and other soil processes. Titanium, which is also a high-field strength element, is present in much higher concentrations and is minimally mobile [*Bern et al.*, 2015]. Tau concentrations were calculated at all horizons within soil profiles, and then depth-weighted averages were calculated for each profile. Complete chemistry data from soil profiles and parent material samples are available in the supporting information.

3. Results

3.1. Parent Material Elemental Chemistry

Parent material samples show notable similarities in elemental chemistry despite representing two distinct sample targets: (1) loess buried at ~4 m depth in soil profiles at Lake Benmore in the southernmost region of the study area and (2) freshly sampled fine overbank deposits from glacial outwash near the outlet of the Tasman Glacier in the northern most region of the study area (Table 1). While fresh outwash sediments have slightly higher base cation concentrations than do buried loess samples, the coefficient of variation for these parent material samples is within or less than analytical uncertainty (CV = 5% for major elements and 3% and 1% for titanium and zirconium concentrations, respectively). Therefore, these loess and outwash sediments provide a reasonable estimate of the parent material for the fine loessal soils across our climate gradient.

3.2. Soil Chemistry and Weathering

Depth-weighted average tau values, which index gains and losses relative to parent material, in general become more negative with rainfall for major monovalent and divalent cations (Figure 2a). Tau-Ca values range from −0.06 to −0.73, indicating that 6–73% of Ca has been lost during weathering of loess parent material and soil development (Table 2). Similarly, data show average net Mg losses ranging from 7 to 56% depending on rainfall. In general, Ca and Mg appear more depleted than Na and K, with mean Ca, Mg, Na, and K losses (mean standard error) of 36 ± 3%, 32 ± 2%, 4 ± 2%, and 9 ± 2%, respectively. These relative elemental losses are consistent with parent material mineralogy and the decreasing weatherability of Ca and Na-plagioclase, K-feldspar, and muscovite. Tau values for these cations are surprisingly constant with

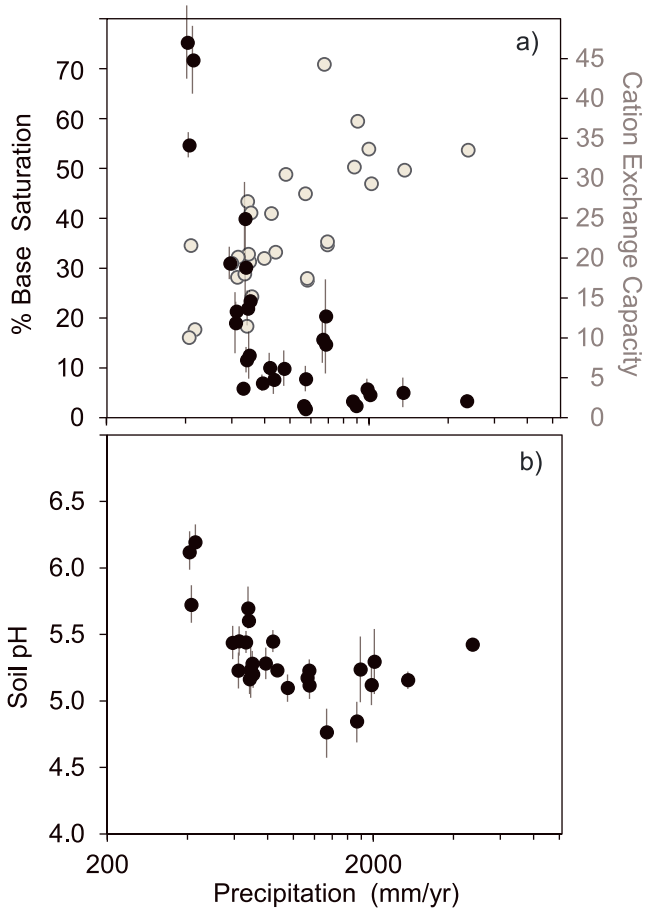

Figure 4. (a) Depth-weighted averages of base saturation decrease (closed circles; left axis) and cation exchange capacity increase (open circles; right axis) with increasing precipitation. Nonlinear changes are coincident with decreases in soil pH (b) at precipitation values around 800 mm/yr. Logarithmic *x* axes highlight how chemical changes occur across a narrow range in pH.

depth in soil profiles, with coefficient of variations for tau Ca averaging 3% (ranging from 1.1 to 9.7%; based on standard errors/depth-weighted averages). These within-profile differences in soil chemistry are greatly exceeded by differences between depth-weighted averages across the climate gradient. Complete profile data are provided in the supporting information.

Pools of exchangeable monovalent and divalent cations also vary strongly across the climate gradient (Figure 2b). Exchangeable Ca, Mg, and K show rapid losses as mean annual precipitation increases from about 400 to 800 mm/yr. In soils that lie beyond ~800 mm/yr precipitation, these cations are largely depleted from exchange sites. For example, pools of exchangeable Ca decrease roughly tenfold (from 9.0 to as little as 0.8 meq/100 g) with increasing precipitation, stabilizing to low values (~1 meq/100 g) at mean annual precipitation >800 mm/yr. Loss of exchangeable cations accompanies observable increases in cation exchange capacity (Figure 4a), decreases in base saturation (Figure 4a), and decreases in pH (Figure 4b) with increasing precipitation. Declining pools of total and exchangeable cations with increasing precipitation (Figures 3 and 4) indicate intensified weathering with increased moisture availability.

Depth-weighted averages for plant-available phosphorus (P), represented by resin-extracted P, decrease with increasing mean annual precipitation (Figure 5) similar to the patterns seen in exchangeable cations, although the decline occurs over a slightly greater range of rainfall. Plant-available P decreases from values as high as 37 ppm at dry sites to <5 ppm in soils receiving >800 mm/yr. Furthermore, Figure 5 demonstrates that at higher rainfall, plant-available P becomes increasingly enriched in surface layers of soil profiles, with as much as 8 times enrichment in the surface relative to the subsoil. This pattern of enhanced P in the surface horizons becomes more evident as overall plant-available P declines.

3.3. Mobility of Iron and Aluminum

The trivalent metallic ions Fe and Al have lower mobilities than the monovalent and divalent ions and often show redistributions within profiles rather than simple profile gain and loss patterns [*Chadwick et al.*, 1990]. Pedogenic iron and aluminum concentrations in the New Zealand soils, separated by dithionite citrate bicarbonate (DCB) and ammonium oxalate extractions, vary as a function of both soil depth and mean annual precipitation. Dithionite-extracted Fe reflects total pedogenic Fe, while oxalate-extractable Fe and Al represent metals bound in short-range order or poorly crystalline mineral forms. The wettest sites show notable subsurface peaks in concentrations of Fe_{DCB} (Figure 6a), $Fe_{oxalate}$ (Figure 6b), and $Al_{oxalate}$ (not shown). In general, concentrations of pedogenic Fe in soils increase with increasing rainfall. Depth-weighted concentrations confirm this increase in total pedogenic Fe and poorly crystalline Fe and Al across the climate gradient

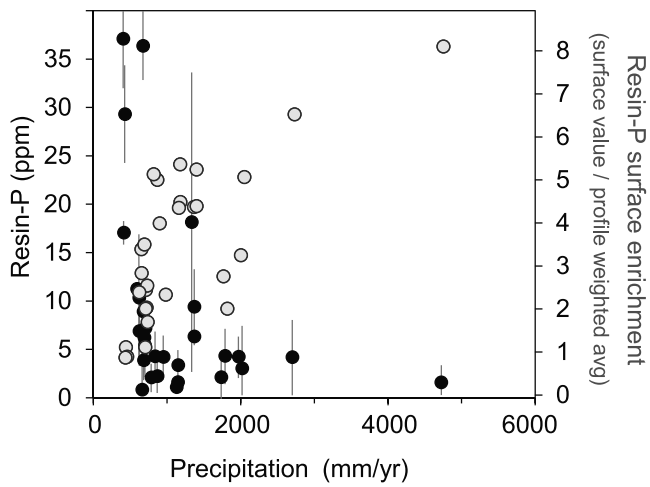

Figure 5. Resin-extractable phosphorus (depth-weighted averages, black circles) decreases with increasing mean annual precipitation, similar to patterns seen for base cations (Figure 2b). The large error bars (standard error) highlight the variability of P with depth. As precipitation increases, this decreasingly abundant plant-available P becomes concentrated in surface horizons (grey circles, second *y* axis; values >1 indicate the surface enrichment relative to the average profile concentration).

(Figure 7a). Increasing amounts of Fe_{DCB} indicate that the higher rainfall soils have undergone greater weathering release of iron than drier sites. On average, approximately 47% of the pedogenic Fe are held in poorly crystalline compounds (as calculated by the ratio of $Fe_{oxalate}/Fe_{DCB}$), and this fraction increases from ~32 to 60% as precipitation increases.

Data from trivalent metallic oxides indicate increasing Al and Fe release, rather than loss, since in general, these elements are retained in the soils, as illustrated by their tau values near zero (Table 2). While metal release appears to increase more or less linearly with increasing moisture availability (Figure 7a), within-profile mobility does not. Instead, we find rapid increases in mobility and redistribution as precipitation increases as evidenced by an enrichment index (enrichment values <1 indicate surface depletion; Figure 7b) and strong subsurface peaks in extractable Fe (Figures 6a and 6b). Fe and Al mobilities appear coincident with other rapid weathering changes at ~800 mm/yr rainfall and in this case is likely pH controlled (Figure 4b).

While pedogenic Fe generally increases with increasing precipitation, there is some suggestion that this trend may stabilize or even reverse at high rainfall. In Hawaiian soils, Fe extracted by DCB declined above 4000 mm rainfall due to increasingly anoxic conditions in wet soils [*Miller et al.*, 2001; *Thompson et al.*, 2011]. At our sites, Fe_{DCB} values increase sharply up to ~2400 mm and may then decline (Figure 7a); however, only one data point suggests such a change. We do not find evidence of a similar decline in $Fe_{oxalate}$, although the data suggest that concentrations may begin to stabilize at precipitation rates above 2000 mm/yr.

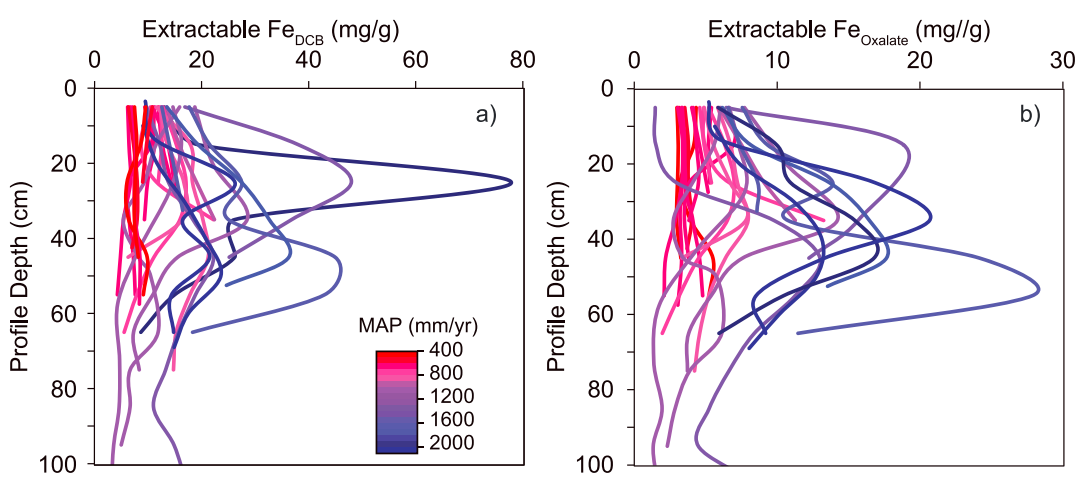

Figure 6. Profiles of Fe_{DCB} and $Fe_{oxalate}$ show the subsurface peaks and higher concentrations of pedogenic iron in wet sites along the precipitation gradient. Profiles are color coded by mean annual precipitation as in Figure 3; dry sites are represented by red lines, and blue lines represent soils at wettest sites.

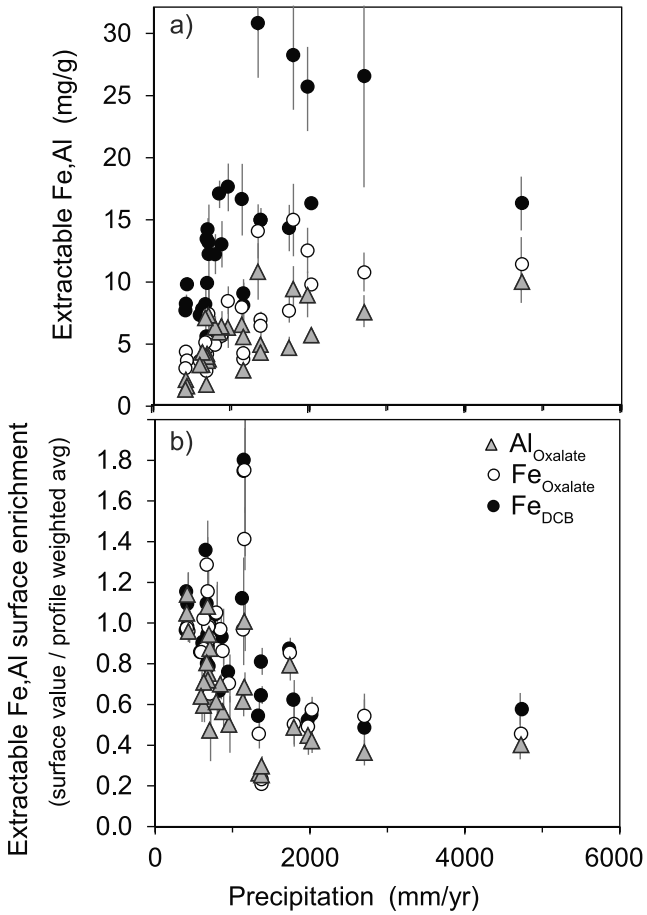

Figure 7. (a) Total pedogenic Fe, measured by dithionite-citrate extractions (Fe_{DCB}), and Al and Fe extracted by ammonium oxalate extractions generally increase with increasing mean annual precipitation. The points correspond to depth-weighted averages from profiles shown in Figure 6, and the error bars represent the standard error. These trivalent metallic oxides become increasingly mobilized downprofile, as shown by (b) the pattern of decreasing surface enrichment values (<1) with rainfall. The values <1 indicate the greater concentration at depth and relative surface depletion.

4. Discussion

4.1. Climate and Moisture Control on Soil Weathering

Results from these New Zealand soils demonstrate that variation in chemical weathering processes and rates are correlated with increasing precipitation across a strong climate gradient. Data show that base cations are released from primary minerals during dissolution and at the same time are stripped from exchange sites. The fate of alkali and alkaline Earth elements held in feldspars and other primary minerals is a sensitive indicator of weathering in young soils [*Porder et al.*, 2007]. Declining pools of total and exchangeable cations with increasing precipitation (Figure 2b) indicate that weathering processes are enhanced by increased leaching power. Weathering dissolves primary minerals and strips these cations from exchangeable surfaces (Figure 3), releasing them to soil waters to eventually be lost downstream. Even at relatively low precipitation, where relatively little Ca is lost (<30%; corresponding to tau values above −0.3), we find marked decreases in the abundance of exchangeable Ca. Cation exchange capacity increases with precipitation (Figure 4a), similar to previously observed patterns from basaltic soils of Hawaii [*Chadwick et al.*, 2003]. The combination of increasing exchange sites and cation leaching (Figure 2b) results in decreasing base saturation (Figure 4a). Under natural conditions this loss of exchangeable Ca and the lack of replenishment by weathering leads to acidification, and we note the rapid loss of cations, and decrease in base saturation occurs at precipitation values of ~800 mm/yr. These changes are coincident with notable decreases in soil pH (Figure 4b) as decreasing pools of base cations means decreased buffering capacity of soils.

We find evidence for an important pedogenic threshold coincident at mean annual precipitation of ~800 mm/yr, which is associated with cation weathering and release, and the rapid mobilization of trivalent metallic ions. Several lines of evidence indicate that this weathering threshold is climate driven and not controlled by other variables. Although the potential variability in parent material composition is likely underconstrained, samples spanning both buried, minimally altered loess from the southernmost region of the study area and glacial outwash in the northernmost region of the study area show close agreement in major element concentrations, suggesting that deposited loess experienced minimal weathering prior to deposition. Furthermore, the observed north to south increase in weathering intensity across the study area is inconsistent with trends that could be explained by parent material age or loess sorting. Moraines underlying loess generally become younger northward, consistent with northward glacial retreat. If soil chemistry reflected disparate ages or distance from glacial sources, then soils would show northward decreasing weathering intensity of soils, reflecting greater leaching with age [e.g., *Dosseto et al.*, 2008]. However, this is not the case.

Instead, it appears that the consistent variation in precipitation strongly overprints other potential confounding controls such as mineralogy and age.

We attribute observed weathering and soil development changes across the New Zealand precipitation gradient to variation in soil moisture availability and leaching intensity. Using climate data from the Ministry of the Environment for New Zealand [*Leathwick et al*., 2002], we compare soil chemistry with annual water deficit, which quantifies the degree to which potential evapotranspiration exceeds water availability. Positive water deficit reflects a negative water balance and low precipitation, while zero deficit reflects a positive water balance. Multiple chemical changes in soils (including net cation weathering losses) scale linearly with local water deficit for sites that are water limited (Figure 8). Plotting annual water deficit versus precipitation, we find that the suggested rainfall threshold of 800 mm/yr is coincident with the transition from an annual water deficit to a positive water balance (Figure 8a). Therefore, the apparent nonlinear control by precipitation on multiple weathering proxies (Figures 2, 4, and 5) is primarily driven by moisture balance, which reflects both the influence of precipitation and evapotranspiration.

A similar threshold behavior has been well documented in basaltic soils of Hawaii [*Chadwick et al*., 2003; *Vitousek and Chadwick*, 2013]. *Chadwick et al*. [2003] also attributed an observable weathering threshold to a transition from negative to positive annual water balance. Although similar geochemical changes occur in both systems, several important differences can be noted between the thresholds observed in Hawaii and the ones we identify in New Zealand. First, the nonlinear increases in soil weathering (based on alkali and alkaline Earth cation depletions) occur at lower mean annual precipitation (MAP) values in soils observed in this paper compared to those in older soils of Hawaii. The threshold differences likely result from several variables intrinsic and extrinsic to the weathering system. A number of factors, including soil hydrology and parent material chemistry, are distinct between the loess-derived New Zealand soils and basalt-derived Hawaii soils. Overall, evapotranspiration is lower in the cool temperate New Zealand landscape than in Hawaii, and hence, more pore volumes of water pass through the soil for the same rainfall. Thus, the transition from negative to positive moisture balance occurs at a lower MAP value in New Zealand soils than in Hawaii. Furthermore, it is possible that the threshold at lower rainfall in New Zealand is a function of parent material chemistry. The New Zealand loess is derived from relatively arkosic greywackes, which offer a less base-rich and less weatherable mineral assemblage compared to Hawaiian basalt and tephra.

A second major difference is that older Hawaiian soils display complete cation (e.g., Ca) depletion with increasing precipitation. Although data from younger New Zealand soils show that there is rapid loss of these elements along the precipitation gradient (Figures 2 and 3), a substantial component of the original cations in rock remain (~40%). We suggest that in Hawaiian soils the changes in chemistry across the rainfall threshold are driven by a transition from kinetic to supply-limited weathering [*Chadwick et al*., 2003; *Vitousek and Chadwick*, 2013]. In contrast, the New Zealand soils remain kinetically limited, even when there is substantial water available to drive leaching losses. Mineralogy may partially explain this difference—some of the primary minerals in New Zealand loess are more recalcitrant to weathering than those in Hawaiian basalt, and the elements they contain may persist in the face of more intense leaching. Soil age may also play an important role in this distinction, as our New Zealand soils have residence times that are at least an order of magnitude younger than the Hawaiian counterparts referenced here. Therefore, both mineral residence time and moisture availability could play important roles in controlling soil chemistry and whether the weathering regime is considered supply or kinetically limited [e.g., *Rasmussen et al*., 2011].

4.2. Implications for Ecology and Biocycling of Nutrients

The observable weathering threshold is important from an ecological and hydrologic perspective. As precipitation increases northward, the pools of plant available nutrients (e.g., Ca, Mg, and P; Figures 2, 3, and 5) become increasingly limited. Furthermore, as phosphorous leaching increases, the remaining plant-available P is concentrated in surface horizons (Figure 5). This surface enrichment results from strong biocycling control on P distribution [*Bullen and Chadwick*, 2016; *Porder and Chadwick*, 2009]. Additionally, redistribution of Fe and Al increases with precipitation across the climate gradient, probably mediated by organic ligands [*Webb et al*., 1986]. $Fe_{oxalate}$ compounds sorb carbon and protect it from microbial decomposition, and therefore, more oxalate extractable compounds suggest greater carbon storage power

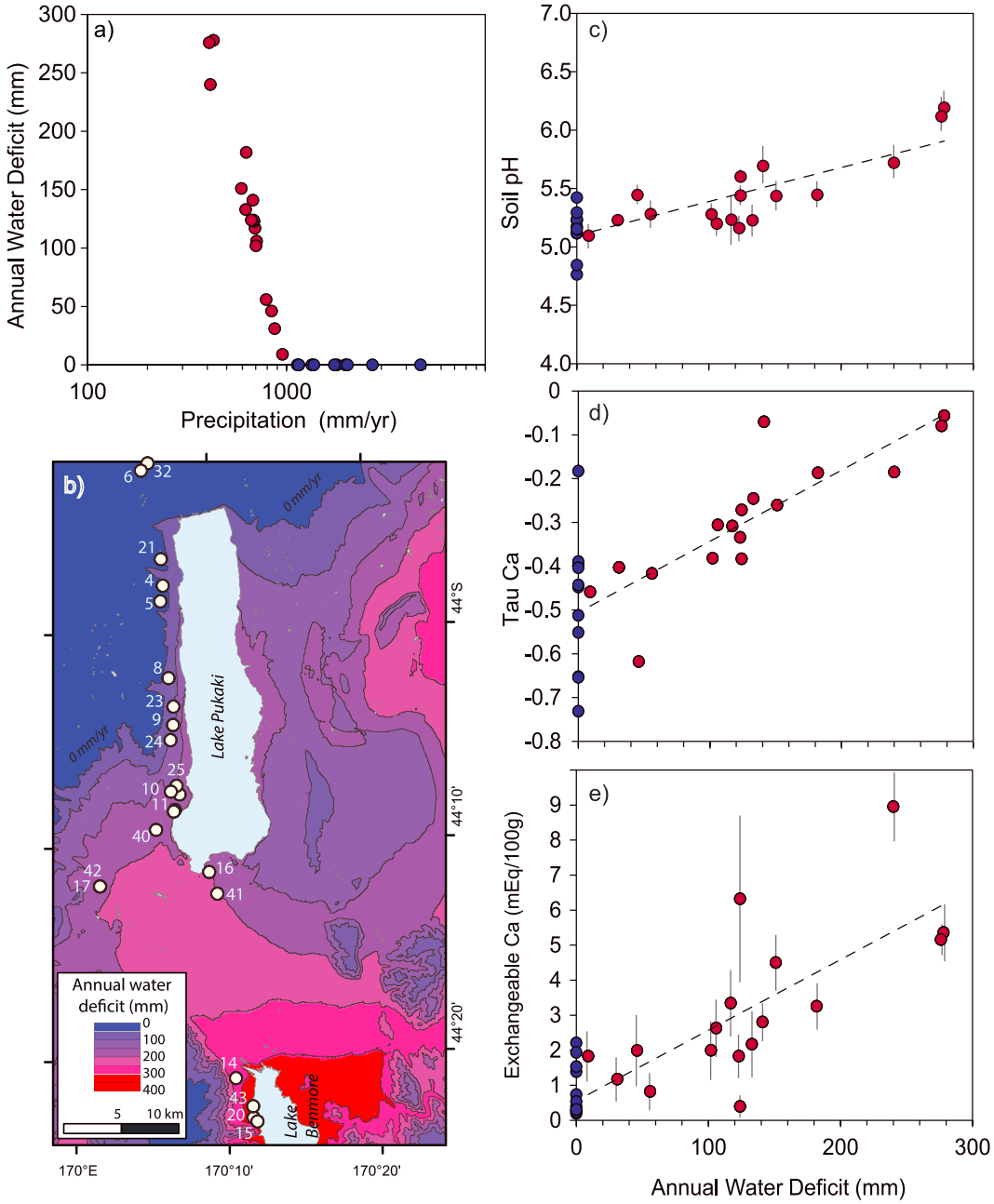

Figure 8. (a) Annual water deficit decreases with increasing precipitation and quantifies the degree to which evaporative demands exceed available soil moisture. Sites with zero water deficit have positive water balance (blue color; precipitation exceeds available moisture), while positive deficit values (purple to red) reflect a negative water balance. (b) Map of annual water deficit for a subregion of the study area where the greatest changes in water deficit are observed. The transition from negative to positive water balance is roughly coincident with the weathering thresholds seen at 800 mm/yr mean annual precipitation across our sites. The nonlinear variations in soil pH, tau Ca, and exchangeable cations observed in previous figures can largely be explained by the transition from positive (blue circles) to negative (red circles) water balance at these sites. (c) Decreases in pH ($r^2 = 0.69$; $p < 0.001$), (d) total calcium depletion ($r^2 = 0.72$; $p < 0.001$), and (e) exchangeable calcium ($r^2 = 0.60$; $p < 0.001$) are strongly coincident with increasing water availability and decreasing water deficits (that occur across a narrow range of precipitation).

[*Kramer et al.*, 2012]. This implies both an ecological control of and impacts from increased metal mobility across the climate gradient [*Lawrence et al.*, 2014]. Redistribution of Fe, Al, and silicate clays have implications for soil hydrology and stability. The development of oxides and clays and their redistribution change water-holding capacity and can affect porosity in ways that lead to changes in water flow patterns with

Table 3. Extractable Element Concentrations

Profile No.	Map 1 (mm)	Extractable Cations (meq/100 g)					CEC (cmol(+)/kg)	Base Saturation (%)	Soil pH	Resin P (μg/g)	Fe and Al Extractions (mg/g)			
		Ca^{2+}	K^{+}	Mg^{2+}	Na^{+}	Sum Cations					Al_{DCB}	Fe_{DCB}	$Al_{oxalate}$	$Fe_{oxalate}$
43	408	5.16	0.39	1.55	0.46	7.56	10.07	75.75	6.1	37.1	1.26	7.71	1.35	3.06
14	414	8.96	0.29	2.33	0.02	11.60	21.59	55.01	5.7	17.1	1.86	8.25	2.11	4.40
15	429	5.36	0.82	1.62	0.06	7.86	11.07	72.18	6.2	29.3	1.72	9.82	1.60	3.67
41	593	4.51	0.34	0.94	0.37	6.16	19.35	31.13	5.4	11.3	4.06	7.34	3.31	3.65
16	623	2.18	0.19	0.60	0.35	3.32	17.61	19.07	5.2	10.3	4.82	7.82	3.32	3.28
19	626	3.26	0.30	0.84	0.05	4.46	20.13	21.46	5.4	6.9	5.55	7.31	4.32	3.47
40	665	0.40	0.32	0.19	0.25	1.16	18.03	5.87	5.4	0.8	5.99	8.21	7.09	5.13
17	677	2.81	0.22	0.67	0.16	3.87	11.50	40.14	5.7	36.4	2.21	5.63	1.73	2.86
13	681	6.33	0.68	1.16	0.38	8.55	27.08	30.30	5.6	8.9	6.70	13.47	3.99	4.67
12	686	1.84	0.24	0.25	0.15	2.48	20.51	11.63	5.2	3.9	6.34	9.93	4.20	4.20
11	693	3.35	0.35	0.46	0.16	4.32	19.55	22.04	5.2	6.2	5.80	14.24	3.64	5.24
25	702	2.00	0.26	0.45	0.42	3.14	25.66	12.56	5.3	5.4	8.08	13.21	7.30	7.44
10	707	2.64	0.20	0.39	0.14	3.37	15.18	23.55	5.2	7.2	5.48	12.24	3.78	4.96
24	788	0.83	0.23	0.25	0.30	1.60	19.98	6.95	5.3	2.1	6.53	12.23	6.35	4.95
9	840	2.00	0.35	0.46	0.15	2.95	25.58	10.06	5.4	4.3	8.23	17.11	5.94	6.02
23	871	1.18	0.19	0.29	0.16	1.82	20.75	7.65	5.2	2.3	7.09	13.03	6.42	5.66
8	953	1.83	0.37	0.55	0.14	2.90	30.48	9.89	5.1	4.2	7.92	17.67	6.31	8.46
5	1132	0.29	0.13	0.10	0.17	0.68	28.07	2.35	5.2	1.1	9.21	16.67	6.54	7.96
21	1149	0.20	0.06	0.09	0.08	0.43	17.47	1.71	5.2	1.6	6.21	9.09	5.57	4.28
4	1152	1.39	0.09	0.16	0.09	1.73	17.24	7.78	5.1	3.4	3.78	8.12	2.88	3.80
6	1337	2.22	2.43	0.88	1.56	7.08	44.27	15.77	4.8	18.2	13.71	30.85	10.81	14.09
32	1373	2.75	0.18	0.60	0.29	3.83	22.04	20.48	-	9.4	5.68	14.99	4.31	6.47
45	1737	0.31	0.29	0.26	0.20	1.05	31.42	3.27	4.8	2.1	5.97	14.35	4.70	7.69
22	1790	0.40	0.19	0.21	0.18	0.97	37.14	2.34	5.2	4.3	11.86	28.27	9.42	15.01
7	1973	1.53	0.21	0.40	0.17	2.31	33.67	5.71	5.1	4.3	12.21	25.72	8.93	12.53
44	2022	0.54	0.26	0.26	0.28	1.34	29.31	4.55	5.3	3.0	7.31	16.34	5.70	9.79
31	2702	0.74	0.12	0.37	0.20	1.43	31.01	5.01	5.2	4.2	9.46	26.58	7.56	10.77
30	4725	0.25	0.14	0.27	0.32	0.98	33.52	3.31	5.4	1.6	9.18	16.36	10.01	11.43

implications for the nature of erosion [e.g., *Lohse and Dietrich*, 2005] and mineral-water interactions [e.g., *Maher*, 2010].

This pedogenic threshold also has significant implications for how climate may modulate weathering release of rock-derived nutrients to ecosystems. Soils at wetter climates are more nutrient depleted and dependent on biocycling than drier ones. We can infer that under changing climates, increases in rainfall and moisture may result in large changes in soil weathering as rock-derived nutrients such as P and Ca are leached rapidly.

4.3. Implications for Climate-Driven Models of Weathering

Despite our focus on climate control in relatively stable soils, we can draw some important conclusions regarding the importance of climate across diverse geomorphic settings. First, the finding that moisture availability is a dominant control on soil weathering in this system is significant and indicates that soil weathering is kinetically limited. Relatively few studies have provided evidence of kinetically limited weathering [*Norton and von Blanckenburg*, 2010; *Rasmussen et al*., 2011] or measured weathering rates in young soils [e.g., *Dixon et al*., 2012; *Larsen et al*., 2014], where the previously discussed, coupled geomorphic-geochemical models suggest that climate may directly affect weathering [e.g., *Ferrier and Kirchner*, 2008]. Our finding of kinetic limitation in New Zealand soils with residence times of ~6 ka indicates that a climate control is indeed discernible across young soils. Considering that several studies have suggested limited climate control on chemical weathering [e.g., *Riebe et al*., 2001], our data provides important constraints to understand if and how climate may influence silicate weathering in mountain environments (Table 3).

These results also provide an important warning about simple weathering regime interpretations based on residence time alone. The nonlinear, threshold behavior of multiple weathering indices with increasing precipitation found here and elsewhere [e.g., *Chadwick et al*., 2003] contrasts with linear models suggested by *White and Blum* [1995]. These geochemical models, used in conjunction with erosion rates in some geomorphic studies [*Dixon et al*., 2009a; *Norton et al*., 2014], predict that small changes in rainfall drive steady changes in soil chemistry. Comparing these linear models with observed data that instead reflect

precipitation threshold-driven changes could result in misinterpretation of findings and misattribution of weathering patterns to other controls.

We find that moisture availability has a strong control on the weathered state of soils. However, the soils studied here are likely kinetically limited even in the wettest sites (with on average 40% of original rock-derived calcium still held within relatively labile minerals). While similar thresholds have been observed in much older soils, including 150 ka and 4 Ma soils in Hawaii [*Vitousek and Chadwick*, 2013], these locations showed near-complete calcium depletion at wettest sites. Based on the fact that we observe this threshold in much younger soils of New Zealand, we propose that this threshold for climate control is likely established early and rapidly during soil formation and can likely persist and even be reinforced over extremely long soil residence times. These results indicate that both moisture availability and soil residence time play important roles in soil and landscape weathering rates [*Rasmussen et al*., 2011], with the transition from negative to positive water balance being a "weathering switch" that can enable rapid weathering. These results also complement recent model-rich studies that suggest that water residence times may be as important as mineral residence times in controlling weathering fluxes [*Maher*, 2010, 2011]. Furthermore, our results caution that understanding climate-weathering interactions requires one to open the hood of the weathering engine (thus understanding the state and mechanics of the soil) rather than simply tracking its speed (by solely measuring rates and indexing net losses).

Our discussion focuses primarily on direct influence of climate on soil weathering; however, other important climatically driven feedback may also be at work in eroding settings. For example, deep chemical weathering may enhance the erodability of soils and diminish surface weathering potential [*Dixon et al*., 2009a]. Climate-enhanced weathering may influence landscape morphology and erosion, especially in moisture-limited systems [*Chadwick et al*., 2013]. Climate may also be a fundamental control on regolith thicknesses [*Goodfellow et al*., 2014], the rates and processes of physical erosion across multiple time scales [e.g., *Bookhagen et al*., 2005], and mountain-range morphologies [e.g., *Montgomery et al*., 2001], which in turn influence how hydrology, morphology, and mineral residence times control weathering processes.

Lastly, the nonlinear, threshold nature of chemical changes with precipitation observed in our study can help shed light on why previous studies may have failed to yield a collective, coherent picture for moisture control on weathering. Chemical changes are observed to occur rapidly over small incremental changes in rainfall and are driven by moisture balance. Therefore, studies that explore narrow climate gradients or that do not capture the transition across this threshold can miss or misinterpret the nature of climate control.

Acknowledgments
The authors owe many thanks to the gracious and knowledgeable station managers that provided both land access and their insights: B. and C. Aubrey at Glen Caim Station, S. and P. Cameron at Ben Ohau Station, M. and G. Seymore at Ferrintosh Station, R. and H. Ivey at Glentanner Station and Katherine Fields, E. Gabriel at Pukaki Downs, and J. Metheral at Totara Peaks. We thank Landcare Research-Manaaki Whenua and the NZ Department of Conservation-Te Papa Atawhai for their guidance and permit assistance. Duane Peltzer, Tim Kerr, Tim Webb, George Hilley, and Peter Almond provided fruitful discussions and support. Field and lab assistance by Zhareen Bulalacao and William Barnes was instrumental, as was field work from Samuel Prentice and Jesse Bateman. Simon Mudd, Craig Rasmussen, and an anonymous reviewer provided helpful comments on this manuscript. This work was funded by NSF ETBC-1019640 and -1020791 (to O.A.C. and P. M.V.). J.L.D. acknowledges support by MT-IOE award from NSF EPS-1101342. Supporting data for this manuscript are included in the supporting information.

References

Amos, C. B., D. W. Burbank, D. C. Nobes, and S. A. Read (2007), Geomorphic constraints on listric thrust faulting: Implications for active deformation in the Mackenzie Basin, South Island, New Zealand, *J. Geophys. Res.*, *112*, B03S11, doi:10.1029/2006JB004291.

Barrell, D. J. A., B. G. Andersen, and G. H. Denton (2011), *Glacial Geomorphology of the Central South Island, New Zealand*, pp. 71, GNS Science.

Berger, G. W., P. J. Tonkin, and B. J. Pillans (1996), Thermoluminescence ages of post-glacial loess, Rakaia River, South Island, New Zealand, *Quat. Int.*, *34*, 177–181.

Bern, C. R., A. Thompson, and O. A. Chadwick (2015), Quantification of colloidal and aqueous element transfer in soils: The dual-phase mass balance model, *Geochim. Cosmochim. Acta*, *151*, 1–18.

Bookhagen, B., R. C. Thiede, and M. R. Strecker (2005), Abnormal monsoon years and their control on erosion and sediment flux in the high, arid northwest Himalaya, *Earth Planet. Sci. Lett.*, *231*(1–2), 131–146, doi:10.1016/j.epsl.2004.11.014.

Brantley, S. L. (2003), 5.03—Reaction kinetics of primary rock-forming minerals under ambient conditions, in *Treatise on Geochemistry*, edited by H. D. H. K. Turekian, pp. 73–117, Elsevier, Oxford, doi:10.1016/B0-08-043751-6/05075-1.

Bullen, T., and O. Chadwick (2016), Ca, Sr and Ba stable isotopes reveal the fate of soil nutrients along a tropical climosequence in Hawaii, *Chem. Geol.*, *422*, 25–45.

Burt, R. (2004), Soil survey laboratory methods manual*Rep* Lincoln, NE.

Chadwick, O. A., and J. Chorover (2001), The chemistry of pedogenic thresholds, *Geoderma*, *100*(3), 321–353.

Chadwick, O. A., G. H. Brimhall, and D. M. Hendricks (1990), From a black to a gray box—A mass balance interpretation of pedogenesis, *Geomorphology*, *3*(3–4), 369–390, doi:10.1016/0169-555X(90)90012-F.

Chadwick, O. A., R. T. Gavenda, E. F. Kelly, K. Ziegler, C. G. Olson, W. C. Elliott, and D. M. Hendricks (2003), The impact of climate on the biogeochemical functioning of volcanic soils, *Chem. Geol.*, *202*(3–4), 195–223, doi:10.1016/j.chemgeo.2002.09.001.

Chadwick, O. A., J. J. Roering, A. M. Heimsath, S. R. Levick, G. P. Asner, and L. Khomo (2013), Shaping post-orogenic landscapes by climate and chemical weathering, *Geology*, *41*(11), 1171–1174, doi:10.1130/g34721.1.

Dahlgren, R., J. Boettinger, G. Huntington, and R. Amundson (1997), Soil development along an elevational transect in the western Sierra Nevada, California, *Geoderma*, *78*(3), 207–236.

Dixon, J. L., and F. von Blanckenburg (2012), Soils as pacemakers and limiters of global silicate weathering, *C. R. Geosci.*, *344*(11–12), 597–609, doi:10.1016/j.crte.2012.10.012.

Dixon, J. L., A. M. Heimsath, and R. Amundson (2009a), The critical role of climate and saprolite weathering in landscape evolution, *Earth Surf. Processes Landforms*, *34*(11), 1507–1521, doi:10.1002/esp.1836.

Dixon, J. L., A. M. Heimsath, J. Kaste, and R. Amundson (2009b), Climate-driven processes of hillslope weathering, *Geology*, *37*(11), 975–978.

Dixon, J. L., A. S. Hartshorn, A. M. Heimsath, R. A. DiBiase, and K. X. Whipple (2012), Chemical weathering response to tectonic forcing: A soils perspective from the San Gabriel Mountains, California, *Earth Planet. Sci. Lett.*, *323–324*, 40–49, doi:10.1016/j.epsl.2012.01.010.

Dosseto, A., S. P. Turner, and J. Chappell (2008), The evolution of weathering profiles through time: New insights from uranium-series isotopes, *Earth Planet. Sci. Lett.*, *274*, 359–371.

Drever, J., K. Murphy, and D. Clow (1994), Field weathering rates versus laboratory dissolution rates: An update, *Chem. Geol.*, *105*, 137–162.

Eden, D. N., and A. P. Hammond (2003), Dust accumulation in the New Zealand region since the Last Glacial Maximum, *Quat. Sci. Rev.*, *22*(18–19), 2037–2052, doi:10.1016/S0277-3791(03)00168-9.

Ewing, S. A., B. Sutter, J. Owen, K. Nishiizumi, W. Sharp, S. S. Cliff, K. Perry, W. Dietrich, C. P. McKay, and R. Amundson (2006), A threshold in soil formation at Earth's arid–hyperarid transition, *Geochim. Cosmochim. Acta*, *70*(21), 5293–5322.

Ferrier, K. L., and J. W. Kirchner (2008), Effects of physical erosion on chemical denudation rates: A numerical modeling study of soil-mantled hillslopes, *Earth Planet. Sci. Lett.*, *272*(3), 591–599.

Ferrier, K. L., J. W. Kirchner, and R. C. Finkel (2012), Weak influences of climate and mineral supply rates on chemical erosion rates: Measurements along two altitudinal transects in the Idaho batholith, *J. Geophys. Res.*, *117*, F02026, doi:10.1029/2011JF002231.

Gabet, E. J., and S. M. Mudd (2009), A theoretical model coupling chemical weathering rates with denudation rates, *Geology*, *37*(2), 151–154.

Goodfellow, B. W., O. A. Chadwick, and G. E. Hilley (2014), Depth and character of rock weathering across a basaltic-hosted climosequence on Hawai'i, *Earth Surf. Processes Landforms*, *39*(3), 381–398.

Hewawasam, T., F. von Blanckenburg, J. Bouchez, J. L. Dixon, J. A. Schuessler, and R. Maekeler (2013), Slow advance of the weathering front during deep, supply-limited saprolite formation in the tropical Highlands of Sri Lanka, *Geochim. Cosmochim. Acta*, *118*, 202–230.

Hilley, G. E., C. P. Chamberlain, S. Moon, S. Porder, and S. D. Willett (2010), Competition between erosion and reaction kinetics in controlling silicate-weathering rates, *Earth Planet. Sci. Lett.*, *293*(1–2), 191–199, doi:10.1016/j.epsl.2010.01.008.

Jenny, H. (1941), *Factors of Soil Formation: A System of Pedology*, McGraw-Hill book Company, Incorporated, New York.

Kerr, T. (2009), *Precipitation Distribution in the Lake Pukaki Catchment, New Zealand*, pp. 376, Univ. of Canterbury, Christchurch.

Kramer, M. G., J. Sanderman, O. A. Chadwick, J. Chorover, and P. M. Vitousek (2012), Long-term carbon storage through retention of dissolved aromatic acids by reactive particles in soil, *Global Change Biol.*, *18*(8), 2594–2605.

Larsen, I. J., P. C. Almond, A. Eger, J. O. Stone, D. R. Montgomery, and B. Malcolm (2014), Rapid Soil production and weathering in the Southern Alps, New Zealand, *Science*, *343*(6171), 637–640, doi:10.1126/science.1244908.

Lawrence, C., J. Harden, and K. Maher (2014), Modeling the influence of organic acids on soil weathering, *Geochim. Cosmochim. Acta*, *139*, 487–507, doi:10.1016/j.gca.2014.05.003.

Leathwick, J., M. Fraser, G. Wilson, D. Rutledge, M. McLeod, and K. Johnson (2002), Land environments of New Zealand: A technical guide edited by M. f. t. Environment, Wellington, New Zealand.

Lohse, K. A., and W. E. Dietrich (2005), Contrasting effects of soil development on hydrological properties and flow paths, *Water Resour. Res.*, *41*, W12419, doi:10.1029/2004WR003403.

Maher, K. (2010), The dependence of chemical weathering rates on fluid residence time, *Earth Planet. Sci. Lett.*, *294*(1), 101–110.

Maher, K. (2011), The role of fluid residence time and topographic scales in determining chemical fluxes from landscapes, *Earth Planet. Sci. Lett.*, *312*(1), 48–58.

McGlone, M. S. (1995), Lateglacial landscape and vegetation change and the Younger Dryas climatic oscillation in New Zealand, *Quat. Sci. Rev.*, *14*(9), 867–881, doi:10.1016/0277-3791(95)00068-2.

McGlone, M. S., A. F. Mark, and D. Bell (1995), Late Pleistocene and Holocene vegetation history, central Otago, South Island, New Zealand, *J. R. Soc. N. Z.*, *25*(1), 1–22, doi:10.1080/03014223.1995.9517480.

Miller, A. J., E. A. G. Schuur, and O. A. Chadwick (2001), Redox control of phosphorus pools in Hawaiian montane forest soils, *Geoderma*, *102*(3–4), 219–237, doi:10.1016/S0016-7061(01)00016-7.

Montgomery, D. R., G. Balco, and S. D. Willett (2001), Climate, tectonics, and the morphology of the Andes, *Geology*, *29*(7), 579–582, doi:10.1130/0091-7613(2001)029<0579:ctatmo>2.0.co;2.

NIWA CliFlo, National climate database, virtual climate station data and products. Retrieved 15 May 2016. [Available at http://cliflo.niwa.co.nz.]

Norton, K. P., and F. von Blanckenburg (2010), Silicate weathering of soil-mantled slopes in an active Alpine landscape, *Geochim. Cosmochim. Acta*, *74*(18), 5243–5258, doi:10.1016/j.gca.2010.06.019.

Norton, K. P., P. Molnar, and F. Schlunegger (2014), The role of climate-driven chemical weathering on soil production, *Geomorphology*, *204*, 510–517.

Porder, S., and O. A. Chadwick (2009), Climate and soil-age constraints on nutrient uplift and retention by plants, *Ecology*, *90*(3), 623–636, doi:10.1890/07-1739.1.

Porder, S., G. E. Hilley, and O. A. Chadwick (2007), Chemical weathering, mass loss, and dust inputs across a climate by time matrix in the Hawaiian Islands, *Earth Planet. Sci. Lett.*, *258*(3), 414–427.

Putnam, A. E., G. H. Denton, J. M. Schaefer, D. J. A. Barrell, B. G. Andersen, R. C. Finkel, R. Schwartz, A. M. Doughty, M. R. Kaplan, and C. Schluchter (2010), Glacier advance in southern middle-latitudes during the Antarctic cold reversal, *Nat. Geosci.*, *3*(10), 700–704.

Raeside, J. D. (1964), Loess deposits of the South Island, New Zealand, and soils formed on them, *N. Z. J. Geol. Geophys.*, *7*(4), 811–838, doi:10.1080/00288306.1964.10428132.

Rasmussen, C., and N. J. Tabor (2007), Applying a quantitative pedogenic energy model across a range of environmental gradients, *Soil Sci. Soc. Am. J.*, *71*(6), 1719–1729.

Rasmussen, C., S. Brantley, D. d. B. Richter, A. Blum, J. Dixon, and A. F. White (2011), Strong climate and tectonic control on plagioclase weathering in granitic terrain, *Earth Planet. Sci. Lett.*, *301*(3–4), 521–530, doi:10.1016/j.epsl.2010.11.037.

Riebe, C. S., J. W. Kirchner, D. E. Granger, and R. C. Finkel (2001), Strong tectonic and weak climatic control of long-term chemical weathering rates, *Geology*, *29*(6), 511–514.

Riebe, C. S., J. W. Kirchner, and R. C. Finkel (2004), Erosional and climatic effects on long-term chemical weathering rates in granitic landscapes spanning diverse climate regimes, *Earth Planet. Sci. Lett.*, *224*(3), 547–562.

Schaefer, J. M., G. H. Denton, D. J. A. Barrell, S. Ivy-Ochs, P. W. Kubik, B. G. Andersen, F. M. Phillips, T. V. Lowell, and C. Schlüchter (2006), Near-synchronous interhemispheric termination of the Last Glacial Maximum in mid-latitudes, *Science*, *312*(5779), 1510–1513, doi:10.1126/science.1122872.

Spörli, K. B., and A. R. Lillie (1974), Geology of the Torlesse Supergroup in the northern Ben Ohau Range, Canterbury, *N. Z. J. Geol. Geophys.*, *17*(1), 115–141.

Stallard, R. F., and J. M. Edmond (1983), Geochemistry of the Amazon: 2. The influence of geology and weathering environment on the dissolved load, *J. Geophys. Res.*, *88*(C14), 9671–9688, doi:10.1029/JC088iC14p09671.

Thompson, A., D. G. Rancourt, O. A. Chadwick, and J. Chorover (2011), Iron solid-phase differentiation along a redox gradient in basaltic soils, *Geochim. Cosmochim. Acta*, *75*(1), 119–133.

Vitousek, P. M., and O. A. Chadwick (2013), Pedogenic thresholds and soil process domains in basalt-derived soils, *Ecosystems*, *16*(8), 1379–1395.

Vitousek, P. M., T. N. Ladefoged, P. V. Kirch, A. S. Hartshorn, M. W. Graves, S. C. Hotchkiss, S. Tuljapurkar, and O. A. Chadwick (2004), Soils, agriculture, and society in precontact Hawai'i, *Science*, *304*(5677), 1665–1669, doi:10.1126/science.1099619.

Waldbauer, J., and C. P. Chamberlain (2005), Influence of uplift, weathering, and base cation supply on past and future CO_2 levels, in *A History of Atmospheric CO_2 and Its Effects on Plants, Animals, and Ecosystems*, edited by I. T. Baldwin et al., pp. 166–184, Springer, New York, doi:10.1007/0-387-27048-5_8.

Walker, J. C., P. Hays, and J. F. Kasting (1981), A negative feedback mechanism for the long-term stabilization of Earth's surface temperature, *J. Geophys. Res.*, *86*(C10), 9776–9782, doi:10.1029/JC086iC10p09776.

Webb, T. H., A. S. Campbell, and F. B. Fox (1986), Effect of rainfall on pedogenesis in a climosequence of soils near Lake Pukaki, New Zealand, *N. Z. J. Geol. Geophys.*, *29*(3), 323–334, doi:10.1080/00288306.1986.10422155.

West, A. J., A. Galy, and M. Bickle (2005), Tectonic and climatic controls on silicate weathering, *Earth Planet. Sci. Lett.*, *235*(1–2), 211–228, doi:10.1016/j.epsl.2005.03.020.

White, A. F., and A. E. Blum (1995), Effects of climate on chemical weathering in watersheds, *Geochim. Cosmochim. Acta*, *59*(9), 1729–1747, doi:10.1016/0016-7037(95)00078-E.

White, A. F., and S. L. Brantley (2003), The effect of time on the weathering of silicate minerals: Why do weathering rates differ in the laboratory and field?, *Chem. Geol.*, *202*(3–4), 479.

White, A. F., A. E. Blum, T. D. Bullen, D. V. Vivit, M. Schulz, and J. Fitzpatrick (1999), The effect of temperature on experimental and natural chemical weathering rates of granitoid rocks, *Geochim. Cosmochim. Acta*, *63*(19–20), 3277–3291, doi:10.1016/S0016-7037(99)00250-1.